

Subdiffusion and dynamical heterogeneities in a lattice glass model

Eric Bertin,^{1,2} Jean-Philippe Bouchaud,² and François Lequeux³

¹ Department of Theoretical Physics, University of Geneva, CH-1211 Geneva 4, Switzerland

² SPEC, CEA Saclay, F-91191 Gif-sur-Yvette Cedex, France

³ ESPCI, 10 rue Vauquelin, F-75005 Paris, France

(Dated: December 2, 2024)

We study a kinetically constrained lattice glass model in which local densities are globally conserved, but randomly redistributed on neighbouring sites. Redistribution is inhibited at high densities. The full steady-state distribution can be computed exactly in any space dimension d , as a function of a parameter encoding the attractive or repulsive nature of the interactions between particles. Dynamical heterogeneities are characterized by a length scale that diverges when approaching the critical density. Interestingly, the motion of mobile regions is found to be subdiffusive for a large range of parameters. The glassy dynamics of the model can be described as a reaction-(sub)diffusion process for the mobile regions.

PACS numbers: 75.10.Nr, 02.50.-r, 64.70.Pf

A common picture of glassy dynamics is that the system reaches progressively deeper and deeper energy states, thus slowing down strongly the dynamics. This picture assumes that energy, and therefore temperature, are the dominant effects governing the physics of glass forming materials. Although this is probably true in many fragile glasses [1], this is not necessarily the case for all systems. For example colloids, or granular materials, also exhibit glassy dynamics associated to jamming: density, rather than temperature, is the dominant effect. A fruitful path, which has attracted considerable attention in recent years, is to introduce “Kinetically Constrained Models” (KCMs) without energy, or with a simple (usually one body) hamiltonian, that take into account sterical constraints through kinetic rules that forbid some transitions between microscopic states [2, 3]. This can be interpreted as a rather natural approach for non hamiltonian jamming systems (in relation to the concept of dilatancy), or as a binarisation of energy barriers in hamiltonian systems (barriers either vanish or diverge).

In this Letter, we consider the model first introduced in [4], which belongs to the above family of KCMs, but where the local variable is the density, which is continuous rather than discrete as in most studied KCMs. The interest of the present model compared to previously studied KCMs is three-fold. First, even though the statistics of the model is non trivial, one can compute exactly the stationary N-body distribution, which turns out to be factorizable for all values of a parameter that describes (repulsive or attractive) interactions between particles, and which has no counterpart in other KCMs. Second, the defect induced mobility for high densities can be studied in details, and the single defect motion is found to be non trivial, i.e subdiffusive, due to a self-induced trapping mechanism (not introduced by hand in the model). Third, dynamical heterogeneities with a rather rich spatial structure are observed.

The model is defined on a lattice of arbitrary dimen-

sion d with N sites. In each cell surrounding lattice site i , a continuous density of particles ρ_i is introduced. The dynamics, aimed at describing density fluctuations, corresponds to a local redistribution of particles across the links of the lattice. At each time step $\Delta t = \tau_0/N$ (τ_0 is a microscopic time scale), a link (j, k) is picked up at random; the corresponding densities ρ_j and ρ_k are redistributed into ρ'_j and ρ'_k , according to:

$$\rho'_j = q(\rho_j + \rho_k), \quad \rho'_k = (1-q)(\rho_j + \rho_k), \quad 0 < q < 1 \quad (1)$$

such that the mass $\rho_j + \rho_k$ is conserved at each step. The fraction q is itself a random variable, distributed according to a distribution $\psi(q)$ such that $\psi(1-q) = \psi(q)$, that plays the role of internal noise in the model. We also want to take into account the fact that a locally dense packing is blocked unless some low density cell is present in its vicinity. This can be done through the introduction of kinetic constraints; a simple constraint is to allow redistributions only if $\rho_j + \rho_k < 2\rho_{th}$, introducing a threshold density ρ_{th} above which the system is no longer able to reorganize locally –in the following, $\rho_{th} = 1$. One can then expect that if the overall density is high, the dynamics slows down dramatically, hence exhibiting a glassy behavior. If one starts from an initial condition such that for all i , $\rho_i^0 < 2$, the evolution rules cannot generate densities $\rho_i > 2$. In order to find an exact solution for the stationary state, we choose a beta distribution $\psi(q) = \Gamma(2\mu)/\Gamma(\mu)^2[q(1-q)]^{\mu-1}$. The case $\mu = 1$ corresponds to a uniform redistribution and may be thought of as non interacting particles (except from their hard-core repulsion). The case $\mu < 1$ favors q close to zero or to one, and can be interpreted as an effective attractive interaction with a phase separation, hindered by steric constraints. Conversely, the case $\mu > 1$ favors the maximal mixing value $q = 1/2$, and mimics repulsive interactions where density fluctuations are reduced.

Considering the master equation describing the model, one can show that a non trivial form of detailed balance

holds [5] –see also [6]. The stationary N -site distribution for a given value of the average density $\bar{\rho}$ then reads:

$$P_{st}(\{\rho_i\}) = \frac{1}{Z_N(\bar{\rho})} \prod_{i=1}^N [\rho_i^{\mu-1} \theta(2 - \rho_i)] \delta \left(\sum_{i=1}^N \rho_i - N\bar{\rho} \right) \quad (2)$$

Such an explicit solution is of great interest, as it shows that the probability distribution is generally not uniform among the available states (except for $\mu = 1$), contrary to an Edwards-like hypothesis, often used for generic jamming problems. Note that this steady-state distribution is obtained in the long time limit only if, as noted above, all the initial densities $\{\rho_i^0\}$ are less than 2 and also if at least some links initially satisfy $\rho_j^0 + \rho_k^0 < 2$ (otherwise no redistribution can occur at all).

From Eq. (2), the ‘canonical’ distribution $P_{can}(\{\rho_i\})$ describing a subpart, with K sites, of the whole system, can be derived in the limit $1 \ll K \ll N$ [5]:

$$P_{can}(\{\rho_i\}) = \frac{1}{Z_N^{can}(\beta)} \prod_{i=1}^K [\rho_i^{\mu-1} \theta(2 - \rho_i) e^{\beta \rho_i}] \quad (3)$$

where β is a thermodynamical parameter conjugated to $\bar{\rho}$. The one-site density distribution is thus given by:

$$p(\rho) = c \rho^{\mu-1} e^{\beta \rho}, \quad 0 < \rho < 2 \quad (4)$$

where c and β are determined from the normalization and the average density $\bar{\rho}$. In order to characterize more quantitatively the glassy properties of this model, it is of interest to compute the fraction η of mobile links, defined as links (j, k) such that $\rho_j + \rho_k < 2$. This quantity η can be rather naturally interpreted as a measure of the degree of glassiness, since the relaxation time is expected to diverge if $\eta \rightarrow 0$. In the ‘canonical’ steady state, η is computed as: $\eta = \int_0^2 d\rho_1 \int_0^2 d\rho_2 p(\rho_1) p(\rho_2) \theta(2 - \rho_1 - \rho_2)$ and can be evaluated numerically. One can easily show that $\eta \rightarrow 1$ in the limit $\bar{\rho} \rightarrow 0$, since the kinetic constraint does not play any role in this case. In the more interesting limit $\bar{\rho} \rightarrow 2$, an asymptotic expression can be derived:

$$\eta \simeq \frac{2 \Gamma(\mu)^2}{(2 - \bar{\rho}) \Gamma(2\mu)} e^{-2/(2 - \bar{\rho})} \quad (5)$$

Thus the fraction of mobile links decreases very fast for $\bar{\rho} \rightarrow 2$, but does not become zero for any average density $\bar{\rho} < 2$, which suggests that the critical density in this model is $\bar{\rho}_c = 2$. This situation is indeed reminiscent of what happens in the Kob-Andersen model [7] in $d = 2$, in which the diffusion coefficient D goes to 0 with the particle density ρ as: $\ln D \sim (1 - \rho)^{-1}$ [8].

All the above analytical results concerning static quantities are valid in arbitrary dimension d . In the following, we present detailed numerical simulations of dynamical quantities in dimension $d = 1$, and discuss briefly the case $d = 2$, where dynamical quantities seem to

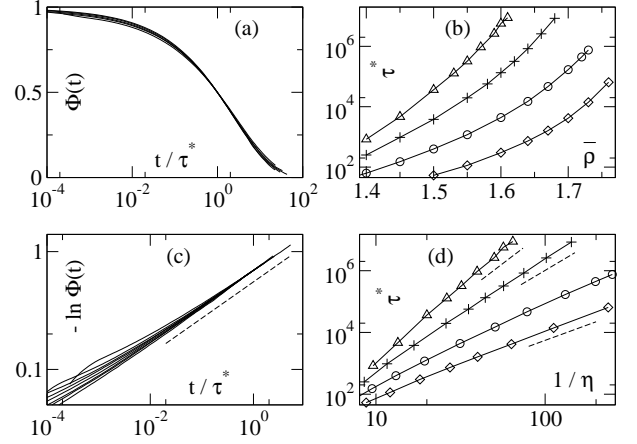


FIG. 1: (a) Time correlation $\Phi(t)$ versus t/τ^* for $\bar{\rho} = 1.60$ to 1.72 ($\mu = 1$). (b) τ^* as a function of $\bar{\rho}$, for $\mu = 0.3$ (\diamond), 1 (\circ), 2 (+) and 3 (\triangle). (c) Stretched exponential behavior of $\Phi(t)$ with $\mu = 2$, and exponent ν determined from $r^2(t)$ (dashed). (d) Dynamic scaling τ^* versus $\ell = 1/\eta(\bar{\rho}, \mu)$ (same symbols as (b)); dashed: exponent $z = 1/\nu$ ($z = 2$ for $\mu = 0.3$).

have a more complex behavior. The relaxation properties of the model can be quantified by introducing on each site i a time function $\phi_i(t)$, that we choose for simplicity to be the local persistence: $\phi_i(t) = 1$ if ρ_i has not changed in the time interval $[0, t]$, and $\phi_i(t) = 0$ otherwise. One can then introduce a global correlation function $\Phi(t) = [\langle \phi_i(t) \rangle]$, where $\langle \dots \rangle$ and $[\dots]$ denote averages over the sites and the noise respectively. Defining the characteristic decay time τ^* through $\Phi(\tau^*) = 1/2$, one can rescale the data by plotting $\Phi(t)$ against t/τ^* [Fig. 1(a)]. The relaxation time τ^* is plotted as a function of $\bar{\rho}$ for different μ in Fig. 1(b). Interestingly, $\Phi(t)$ behaves as a stretched exponential: $-\ln \Phi(t) \sim (t/\tau^*)^\gamma$, as seen on Fig. 1(c). The exponent γ matches perfectly the prediction $\gamma = \nu$, where ν is defined from the sub-diffusion of mobility defects: $r^2(t) \sim t^{2\nu}$ –see below.

A further question of interest is to know whether some non trivial (growing) length scale can be associated with the approach of the glass transition as $\bar{\rho} \rightarrow 2^-$. Since the probability distribution is factorized, no static correlation length can grow in this regime. Thus such a length scale can only appear in dynamical quantities, such as four point correlation functions that have been of great interest recently to describe dynamical heterogeneities [9, 10, 11, 12]. In physical terms, these dynamical heterogeneities can be interpreted as the onset of ‘fast’ and ‘slow’ regions in the system, with a typical size which is growing when the glass transition is approached. More precisely, one can introduce on each site i a local variable $\phi_i^* \equiv \phi_i(\tau^*)$, leading to a natural definition of ‘slow’ and ‘fast’ regions, which then correspond to $\phi_i^* = 1$ and $\phi_i^* = 0$ respectively. This particular choice of ϕ_i^* ensures that fast and slow regions occupy comparable volumes.

There are various ways to identify quantitatively the

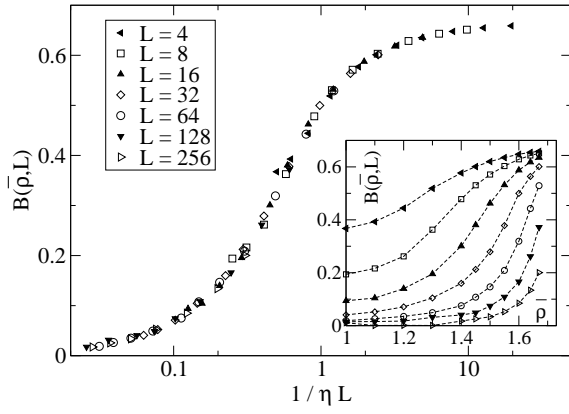


FIG. 2: Inset: plot of $B(\bar{p}, L)$ as a function of \bar{p} for different values of L ($\mu = 1$). The curves do not cross, except presumably for $\bar{p} = 2$. Main plot: $B(\bar{p}, L)$ plotted as a function of the rescaled variable $1/(\eta L)$. The collapse is very good, showing that the characteristic length scale ℓ is proportional to the inverse of the concentration η of mobile links.

characteristic length scale ℓ of these dynamical heterogeneities. Following Berthier [10], one can study the fourth (Binder) cumulant $B(\bar{p}, L)$ of the random variable $\omega \equiv L^{-d} \sum_i \phi_i^*$, where the sum is on all the sites of a finite system of linear size L . This quantity, which measures the ‘non-Gaussianity’ of ω , is zero for $\ell \ll L$ and equal to a certain constant (2/3 with Binder’s normalization) for $\ell \gg L$. Using finite size scaling arguments, one expects $B(\bar{p}, L)$ to scale as a function of ℓ/L . We indeed find in the present model that all data rescale perfectly when plotted as a function of $1/(\eta L)$ [Fig. 2], showing that ℓ is in fact simply the average distance $1/\eta$ between mobile links. It is then rather natural to look for a scaling relation between the relaxation time τ^* and the length ℓ of the form $\tau^* \sim \ell^z$, where z is a dynamical critical exponent; τ^* is plotted as a function of $\ell = 1/\eta$ on a log-log scale in Fig. 1(d). Interestingly, the relation between τ^* and ℓ depends strongly on μ ; for $\mu = 0.3, 2$ and 3, the data are well fitted by power laws for $\ell \gg 1$, whereas for $\mu = 1$, a systematic curvature appears.

To understand these results, it is of interest to introduce a qualitative description of the high density dynamics in terms of reaction-diffusion of mobility excitations [13]. When a redistribution occurs on a given link, its ‘state’ (mobile or not) cannot change, due to mass conservation. However, neighboring links *can* change state since the mass associated to these links is not conserved in this redistribution. So it is possible to create or annihilate a mobile link when it shares a site with another mobile link. Denoting a mobile link by A and an immobile one by \emptyset , one can write schematically these processes as $(A, \emptyset) \rightarrow (A, A)$ and $(A, A) \rightarrow (\emptyset, A)$, whereas the simple annihilation process $A \rightarrow \emptyset$ is forbidden by the conservation rule. Moreover, a chain of two such processes is equivalent to the motion of a ‘defect’ A . At high

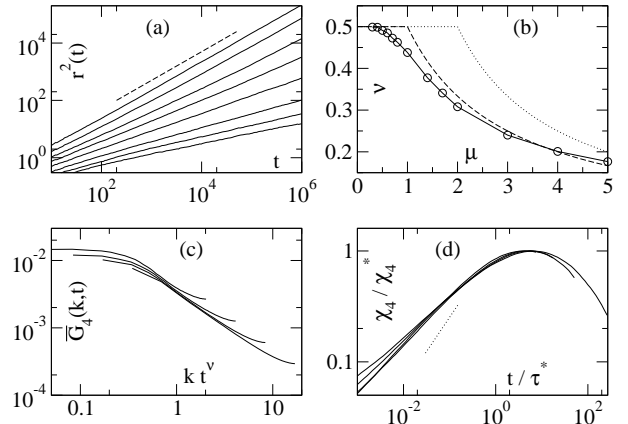


FIG. 3: (a) Mean-square displacement $r^2(t)$ for $\mu = 0.3, 0.6, 1, 1.4, 2, 3, 4$ and 5 (top to bottom) and $\bar{p} = 1.75$; dashed: slope 1. (b) Exponent ν defined by $r^2(t) \sim t^{2\nu}$ (\circ), annealed (dotted) and quenched (dashed) barrier models predictions. (c) Rescaled correlation $\bar{G}_4(k, t)$ against $k t^\nu$ ($\bar{p} = 1.60, \mu = 2$). (d) Rescaled susceptibility $\chi_4(t)/\chi_4^*$ versus t/τ^* for $\bar{p} = 1.50, 1.55, 1.58$ and 1.60 ($\mu = 2$); dots: slope 2ν .

density \bar{p} , i.e. at low concentration of mobility, branching and annihilation of mobility excitations become rare, and mobility motion is the dominant relaxation mechanism (for a related discussion, see [14]).

If the mobility excitations had a purely diffusive motion, say $r^2(t) \sim Dt$, with a diffusion constant D which does not vanish when $\bar{p} \rightarrow 2$, τ^* would scale with ℓ as $\tau^* \sim \ell^2$, i.e. $z = 2$. This scaling law is not compatible with the data shown in Fig. 1(d) as soon as $\mu \geq 1$. Such a discrepancy could come from the \bar{p} dependence of the diffusion constant D , as in the Fredrickson-Andersen (FA) model in $d = 1$, where D depends on temperature, leading to $z = 3$ [11]. However, the main mechanism at play in the present model is different, and related to a genuine subdiffusive motion of individual defects. We show in Fig. 3(a) the mean-square displacement $r^2(t)$ of mobility excitations for several values of μ . The motion of mobility is found to be subdiffusive for a whole range of parameter μ , which can be estimated to be $\mu \gtrsim 1$ (finite time effects induce a rather strong uncertainty on this threshold). The exponent ν characterizing the asymptotic power law regime $r^2(t) \sim \tilde{D}(\bar{p}) t^{2\nu}$ is shown in Fig. 3(b) and is found to be independent of \bar{p} at high density. From this relation, one deduces that $\ell^2 \sim \tilde{D}(\bar{p}) \tau^{*2\nu}$; neglecting the variations of $\tilde{D}(\bar{p})$ with respect to that of τ^* , one finds $z = 1/\nu$. Using the measured values of ν , one can compare this prediction with the direct evaluation of z on Fig. 1(d) for $\mu = 2$ and 3 (dashed lines). The agreement is quite good, although some discrepancies, presumably due to the variations of \tilde{D} , appear. For $\mu = 0.3$, one recovers the standard exponent $z = 2$.

Besides, this subdiffusive motion of mobility accounts very well for the stretched exponential behavior of $\Phi(t)$.

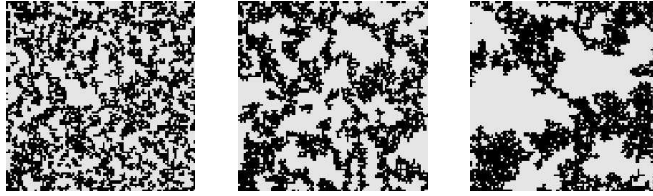


FIG. 4: Direct visualization of dynamical heterogeneities with the variables ϕ_i^* , for $\bar{\rho} = 1.50, 1.65, 1.75$, in a system of size $N = 100^2$ ($\mu = 1$). Only black sites ($\phi_i^* = 0$) have changed state between $t = 0$ and $t = \tau^*$. The typical size of both types of regions clearly increases with density.

At short time ($t \ll \tau^*$), the correlation behaves as $1 - \Phi(t) \sim r(t)/\ell$, i.e. as $r(t) \sim t^\nu$. Thus $\Phi(t)$ should be well approximated by a stretched exponential with exponent ν , which indeed matches perfectly the numerical data –see Fig. 1(c). Interestingly, the dynamics of mobility can be mapped onto a one-dimensional barrier model [15], since the processes $(\emptyset, A, \emptyset) \rightarrow (\emptyset, A, A)$ and $(\emptyset, A, \emptyset) \rightarrow (A, A, \emptyset)$ involve waiting times which become broadly distributed when $\bar{\rho} \rightarrow 2$ [5]. Since there is no quenched disorder in the model, one may expect to observe essentially an annealed dynamics, where each barrier is drawn anew at random once overcome. This would yield a subdiffusion exponent $\nu = 1/\mu$ for $\mu > 2$ [5, 15], which actually does not match the numerical data [Fig. 3(b)]. But as the environment of a mobile link is frozen for times of the order of τ^* , the quenched barrier model might be of some relevance to the present situation. Indeed, the corresponding exponent $\nu = 1/(1 + \mu)$ for $\mu > 1$ is in rather good agreement with the numerics. So the existence of slow regions induces non trivial correlations, and mimics the presence of quenched disorder, which is actually ‘self-generated’ in this model.

Another important quantity is the spatio-temporal (four-point) correlation function $G_4(r, t)$ defined as:

$$G_4(r, t) = [\langle \phi_i(t) \phi_{i+r}(t) \rangle - \langle \phi_i(t) \rangle \langle \phi_{i+r}(t) \rangle] \quad (6)$$

Introducing the Fourier transform $\tilde{G}_4(k, t)$ of $G_4(r, t)$, one expects the rescaled correlation $\overline{G}_4(k, t) \equiv \tilde{G}_4(k, t)/(t^\nu G_4(r = 0, t))$ to scale as a function of $k t^\nu$ [16]. The corresponding data are plotted on Fig. 3(c), showing a reasonable collapse. Integrating $G_4(r, t)$ over r yields the dynamical susceptibility $\chi_4(t)$ which has been shown to encode important information on the dynamics of the system [16]. Fig. 3(d) displays $\chi_4(t)/\chi_4^*$ versus t/τ^* for different $\bar{\rho}$, where χ_4^* is the maximum of $\chi_4(t)$, and τ^* has been determined from $\Phi(t)$. The resulting collapse is rather good, although very long time data would be needed to really test the collapse for $t \gg \tau^*$. At short time ($t \ll \tau^*$), data converge very slowly when $\bar{\rho} \rightarrow 2$ to the predicted power law $\chi_4(t) \sim t^{2\nu}$ [16], indicating strong corrections to the asymptotic form.

Let us now briefly discuss the qualitative behavior of the model in dimension $d = 2$, leaving a fuller account

to Ref. [5]. It is interesting to visualize directly the variables ϕ_i^* for a given realization of the dynamics. This is done on Fig. 4, for densities $\bar{\rho} = 1.50, 1.65$ and 1.75 . The typical size of these ‘fast’ and ‘slow’ regions is clearly seen to increase with $\bar{\rho}$. Note that a strong asymmetry between slow and fast regions appears: slow regions are essentially compact, whereas fast ones seem to develop a fractal structure when their size increases. Numerical results (not shown) indicate that in dimension $d = 2$, the cumulant $B(\bar{\rho}, L)$ cannot be rescaled by the typical distance $\eta^{-1/2}$ between mobility defects. Instead, an approximate rescaling can be obtained using $\ell \sim \eta^{-\alpha}$, with $\alpha \approx 0.35$. Mobility excitations exhibit a subdiffusive regime for $\mu > 1$, which crosses over at large time to a diffusive one, at odds with results observed in $d = 1$.

In summary, we have analyzed a new KCM with a conserved and continuous density field, and a parameter describing the interaction between particles. Although non trivial, the statics of the model can be computed exactly. The dynamics exhibits many interesting features, such as a subdiffusive behavior of mobility excitations. It would be interesting to see how much of this behavior can be analytically understood, at least in one dimension. In this respect, the renormalization group approach advocated in [17] may be considered as a promising path.

- [1] M. L. Ferrer *et. al.*, J. Chem. Phys. **109**, 8010 (1998); G. Tarjus *et. al.*, J. Chem. Phys. **120**, 6135 (2004).
- [2] F. Ritort and P. Sollich, Adv. Phys. **52**, 219 (2003).
- [3] J. P. Garrahan and D. Chandler, Phys. Rev. Lett. **89**, 035704 (2002).
- [4] J. Lopez-Rios, P. M. Billangeon, and F. Lequeux, J. Stat. Mech.: Theor. Exp., P08003 (2004).
- [5] E. Bertin, J.-P. Bouchaud, and F. Lequeux, to be published.
- [6] E. Bertin, O. Dauchot, and M. Droz, Phys. Rev. Lett. **93**, 230601 (2004); cond-mat/0412071.
- [7] W. Kob and H. C. Andersen, Phys. Rev. E **48**, 4364 (1993).
- [8] C. Toninelli, G. Biroli, and D. S. Fisher, Phys. Rev. Lett. **92**, 185504 (2004).
- [9] C. Donati, S. C. Glotzer, P. H. Poole, W. Kob, and S. J. Plimpton, Phys. Rev. E **60**, 3107 (1999).
- [10] L. Berthier, Phys. Rev. Lett. **91**, 055701 (2003).
- [11] L. Berthier and J. P. Garrahan, J. Chem. Phys. **199**, 4367 (2003).
- [12] G. Biroli and J.-P. Bouchaud, Europhys. Lett. **67**, 21 (2004).
- [13] M. Schulz and S. Trimper, J. Stat. Phys. **94**, 173 (1999).
- [14] S. Whitelam, L. Berthier, and J. P. Garrahan, Phys. Rev. Lett. **92**, 185705 (2004).
- [15] J.-P. Bouchaud and A. Georges, Phys. Rep. **195** (1990).
- [16] C. Toninelli, M. Wyart, L. Berthier, G. Biroli, and J.-P. Bouchaud, cond-mat/0412158.
- [17] S. Whitelam and J. P. Garrahan, Phys. Rev. E **70**, 046129 (2004)